Three Dimensional Face Recognition Using Iso-Geodesic and Iso-Depth Curves

Sina Jahanbin, Hyohoon Choi, Yang Liu, Alan C. Bovik

Abstract— **In this paper a new framework for personal identity verification using 3-D geometry of the face is introduced. Initially, 3-D facial surfaces are represented by curves extracted from facial surfaces (facial curves). Two alternative facial curves are examined in this research: iso-depth and iso-geodesic curves. Iso-depth curves are produced by intersecting a facial surface with parallel planes perpendicular to the direction of gaze, at different depths from the nose tip. An Iso-geodesic curve is defined to be the locus of all points on the facial surface having the same geodesic distance from a given facial landmark (e.g. the nose tip). Once the facial curves are extracted, their characteristics are encoded by several features like the shape descriptors or polar Euclidean distances from the origin (nose tip). The final step is to verify or disapprove requests from users claiming the identity of registered individuals (gallery members) by comparing their features using Euclidean distance classifier or support vector machine (SVM). The performance results of the identity verification experiments are reported and a comparison is made between the two alternative curve-based facial surface representations.**

I. INTRODUCTION

A biometric feature is a measurable physiological or behavioral attribute that can be used for automatic recognition of individuals. Since the beginning of civilization, humans have been instinctively using characteristics such as voice and face for recognition purposes; however, the concept of automated biometric systems is relatively new. The emergence of biometric systems coincides with significant advancement in the field of computer processing and availability of low-cost and practical acquisition technologies [1].

In recent years, biometrics has received considerable attention from researchers in various disciplines, government agencies, and private sector industries. The importance of biometric security systems is to the extent that several universities have already established degree programs particularly focusing on the engineering and design of biometric systems [2]. This interest is fueled by the growing demand for automated personal identification in applications ranging from low to high security, including but not limited to access control to buildings, surveillance, airport screening, and smart cards. Improved biometric technologies are expected to replace current, less specific methods such as pin numbers, access codes/cards and radio frequency ID tags which are susceptible to loss or theft. Examples of early deployments within US government include the US-Visit program and the transportation worker identification credentials (TWIC) program [3].

Several biometrics have been deployed for automatic identification including fingerprints, facial images, iris scans, gait, retina, and facial thermograms. Although biometrics such as fingerprints and iris scans have begun to yield reliable performance, the human face remains the most attractive biometrics because of its unique advantages. Facial images are easily acquired with commonly available sensors (cameras) without the need for physical contact (non-intrusive acquisition). It requires minimum cooperation and does not raise any health issues. For instance, fingerprint measurement raises health and social concerns related to touching a sensor used by countless individual. Iris scans are difficult to capture and general public has inherent fears related to “scanning" the eyes with a light source [4].

II. RELATED WORK

The majority of effort in early days of face recognition was focused on using 2-D (luminance) facial images. While several sophisticated 2-D solutions have been proposed, unbiased evaluation studies show that their collective performance remains unsatisfactory, and degrades significantly with variation in lighting, face position, or non-neutral facial expressions [5]. However, newly-developed 3-D face scans encode the anatomical structure of the face, and hence are independent of ambient illumination conditions and pose variations. Using 3-D information has great potential to overcome the shortcomings of recognition systems based on 2-D images.

Recently, several 3-D face recognition algorithms are proposed in which three dimensional facial surfaces are represented by unions of curves. This trend is mainly motivated because a wealth of techniques are available for curve matching and it is a much more studied problem than the freeform surface matching [6].

One of the earliest curve-based facial surface representations is the “point signature" concept proposed by Chua and Jarvis [7]. For any given landmark on the facial surface (e.g., nose tip or eye corner), a 3-D curve C is extracted by intersecting the surface with a sphere of radius R centered at that landmark. The point signature is defined to be the signed distances between each point on facial curve C and its corresponding projection on plane p fitted to C passing through the centroid.

In [8] Samir *et al.* represented facial surfaces using a union of level-set curves of the depth function with respect to the nose tip (iso-depth curves). Consequently, 3-D facial surfaces

This work was not supported by any organization

S. Jahanbin, Y. Liu, and A. C. Bovik are with the Department of Electrical and Computer Engineering, The University of Texas at Austin, USA jahanbin@ece.utexas.edu

H. Choi is with Samsung Electro-Mechanics R&D Institute, South Korea hyohoon.choi@samsung.com

are implicitly compared by measuring similarity between corresponding planar iso-depth contours. One limitation of the iso-depth curves is that they are very susceptible to changes in gaze direction. Some Euclidean transformations of facial surface such as in-depth rotation of facial surface (inaccurate estimation of gaze direction) result in deformed facial curves that are not the Euclidean transformed versions of the original ones. To mitigate the effect of pose variation in recognition performance, an extremely accurate gaze alignment step is required that proves to be very costly and difficult.

Sun *et al.* [9] introduced a new curve-based 3-D object representation method called the“Point fingerprints" and successfully tested this method in surface registration and matching applications. In this method, surfaces are represented by a set of 2-D contours that are the projection of geodesic circles on a plane tangent to the surface at the center, i.e., a surface landmark. These contours are called point fingerprint because of their similarity to fingerprint patterns. Unlike iso-depth curves [8], point fingerprints are inherently robust against Euclidean transformations such as in-depth rotation and translation of the 3-D surface (pose invariance).

Motivated by the effectiveness and pose-invariance nature of the point fingerprints (also referred to as iso-geodesic curves in this paper), a novel automatic face recognition system is proposed in this paper where 3-D facial surfaces are represented by point fingerprints extracted around automatically pinpointed nose tip. Iso-depth contours [8] are also extracted with respect to the nose tip and their face recognition performance is used as a benchmark for comparison. Curve extraction procedures are explained in section III. Once facial curves are extracted, their appearance is characterized by two type of attributes described in section IV. Firstly, polar Euclidean distances from the nose tip are sampled at multiple angles. Secondly, a combination of commonly used shape descriptors such as ratio of principal axes, convexity, compactness, circular variance, and elliptic variance are calculated as defined in [10].

The validity of a user's request claiming the identity of an enrolled subjects in the access control application is confirmed by comparing features extracted from the user's recently obtained facial scan with those from the registered individual (having access privilege) stored in the memory of the system using state of the art classifiers. One option investigated in this paper is to initially reduce the features' dimensionality using a standard linear discriminant analysis (LDA) procedure followed by verification made by a Euclidean distance decision rule. The second option is training and verification by support vector machines (SVM). SVM is attractive here because it can achieve high classification accuracy using relatively small sets of training samples. SVM works well with high-dimensional data avoiding the “curse of dimensionality" and “small sample size" problems often encountered in designing classifiers for face recognition. Results are presented in section V followed by discussion in section VI.

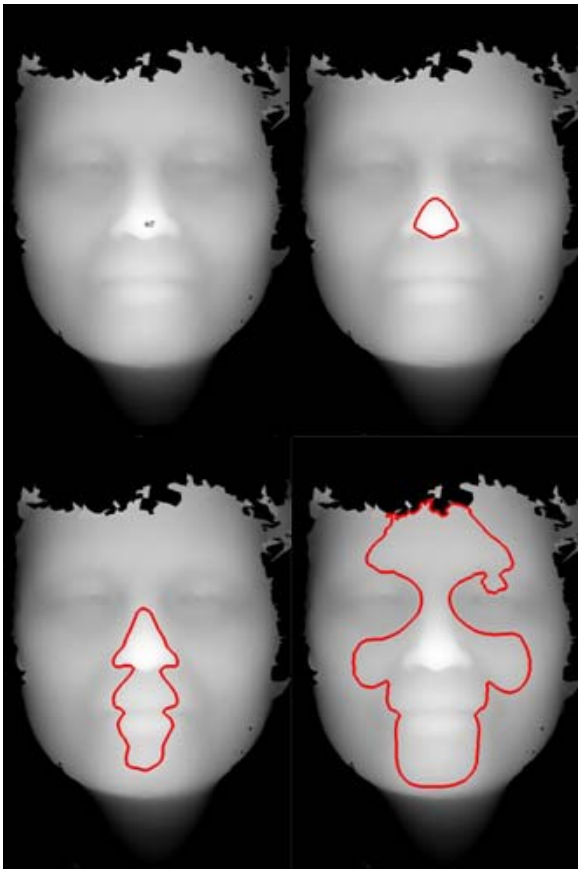

Fig. 1. An Example range image and its corresponding iso-depth curves.

III. CURVE EXTRACTION

In order to extract curves from a 3-D facial image, the first step is to define real-valued functions on that surface [11]. In this paper two real-valued functions are defined on facial surfaces presented by range images: The depth value (z value) and the geodesic distance from the nose tip. Level sets of each function result in closed curves on the facial surface. Fig. 1 shows an example range image where the value of each pixel (z value) represent the distance of that point from the sensor.

A. Iso-Depth Curves

One suitable class of curves capable of capturing the geometric characteristics of 3-D facial surface is the set of contours located at the intersection of a facial surface with parallel planes perpendicular to direction of gaze, at different depths from the nose tip (iso-depth). In this paper, three iso-depth curves are extracted from each range image at empirically selected depth values $z = 25, z = 50$, and $z = 75$. Fig. 1 shows an example range image with the nose tip automatically detected using Gabor filters response method described in [12]. This figure also depicts three iso-depth curves extracted from the same range image.

B. Iso-Geodesic Curves

Another set of facial curves are defined to be the loci of all points on the facial surface having the same geodesic

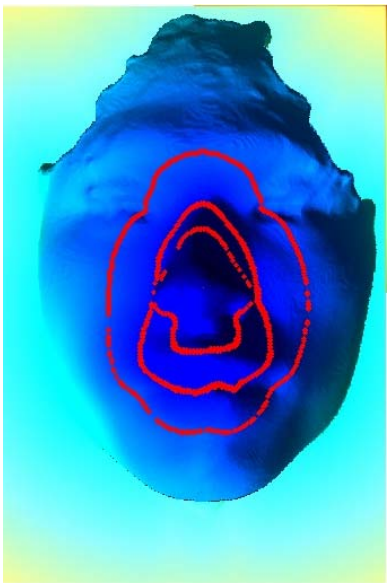

Fig. 2. Example of a range image with iso-geodesic curves marked with red points.

distance to the automatically detected nose tip. The geodesic distance between two points on a surface is the shortest path between these two points along the surface. The main advantage of these iso-metric geodesic curves is their invariance with changes in gaze direction. We have implemented a "fast marching" [13] based algorithm to extract iso-geodesic curves around automatically detected nose tip. Fig. 2 shows a range image with iso-geodesic contours (geodesic circles) corresponding to geodesic distances $d = 65, d = 95$, and $d = 130$ marked with red dots. In this paper, the 2-D projection of these three 3-D curves on $x-y$ plane is utilized to represent the 3-D faces.

IV. FEATURE EXTRACTION

From each iso-depth or iso-geodesic facial curve two sets of features are calculated:

A. Simple Shape Descriptors

Each facial curve is encoded by a set of five primitive shape descriptors widely used in object recognition (Fig. 3) and explained in detail in [10]. These simple shape descriptors are invariant to translation and in-plane rotation around the nose tip. Assuming that each incoming face from the dataset is represented by a set of 3 iso-depth or iso-geodesic curves, a 15 dimensional augmented feature vector is constructed for each curve-based representation by concatenating simple shape descriptors calculated from each curve. These shape features are as follows:

1) Convexity:: The convexity measure of an object is defined to be the ratio between perimeter of its convex hull and the length of its contour (1). A convex hull is the minimum convex covering of an object and can be visualized by imagining an elastic band stretched open to encompass the given object.

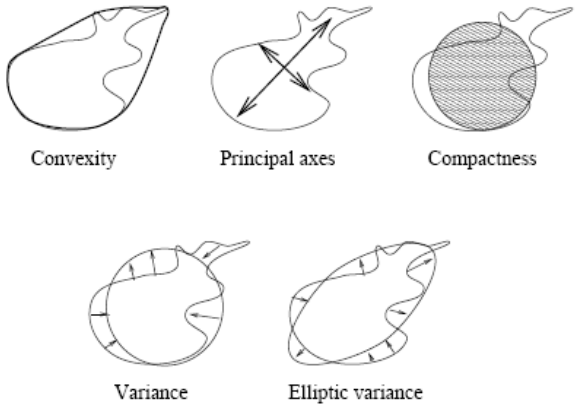

Fig. 3. Five simple shape descriptors [10].

$$conv = \frac{P_{convexhull}}{P} \tag{1}$$

2) Ratio of Principal Axes:: If each point of a curve is considered as an instance of a 2-D random variable, the principal component analysis (PCA) can be used to find the orientation and length of the principle axes. Principal axes are two orthogonal line segments that cross each other in the centroid of the object and represent the directions that possess the maximum variations and zero cross-correlation. The lengths of principal axes equal the eigenvalues $\lambda_{1,2}$ of the covariance metrix C of a contour. Let us denote elements of C as

$$C = \begin{pmatrix} c_{xx} & c_{xy} \\ c_{yx} & c_{yy} \end{pmatrix} \tag{2}$$

the ratio of principal axes is a reasonable measure of elongation and can be calculates directly:

$$prax = \frac{c_{yy} + c_{xx} - \sqrt{(c_{yy} + c_{xx})^2 - 4(c_{xx}c_{yy} - c_{xy}^2)}}{c_{yy} + c_{xx} + \sqrt{(c_{yy} + c_{xx})^2 - 4(c_{xx}c_{yy} - c_{xy}^2)}} \tag{3}$$

3) Compactness:: The compactness measure used in this paper is the ratio of the perimeter of a circle with equal area as the original object and the original perimeter. i.e.,

$$comp = \frac{P_{circle}}{P} = \frac{2\sqrt{A\pi}}{P}, \; A_{circle} = A \tag{4}$$

The compactness measure reaches its maximum in a circular object and reaches zero in thin, complex objects.

4) Circular Variance:: A shape can be compared against a simple and general template such as a circle. The proportional mean-squared error with respect to solid circle, or circular variance, can be defined

$$cvar = \frac{1}{N\mu_r^2} \sum_i (\|\mathbf{p_i} - \boldsymbol{\mu}\| - \mu_r)^2 \tag{5}$$

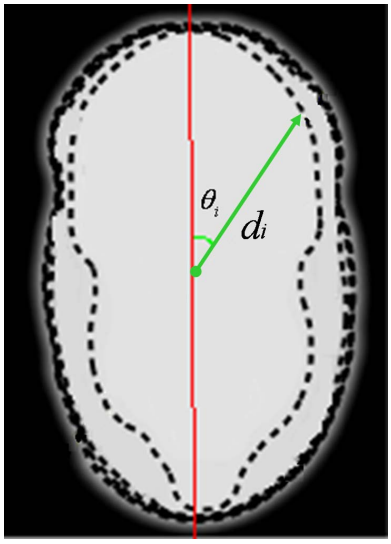

Fig. 4. Polar distances from nose tip to points on facial curve.

where $\mathbf{p_i} = \begin{pmatrix} x_i \\ y_i \end{pmatrix}$ defines the contour points. The centroid of contour points is $\boldsymbol{\mu} = \frac{1}{N}\sum_i \mathbf{p_i}$ while the mean radius is simply $\mu_r = \frac{1}{N}\sum_i \|\mathbf{p_i} - \boldsymbol{\mu}\|$.

Circular variance is zero for a perfect circle and increases along shape complexity and elongation.

5) Elliptic Variance:: Similar to circular variance, objects can be compared to ellipses that are simple and yet enjoying from higher degree of freedom (compared to circles) by allowing elongation. An ellipse is fitted to the shape and mapping error is measured. Intuitively, it seems logical to find an ellipse having an equal covariance matrix, $C_{ellipse} = C$. It is practically effective to apply the inverse approach yielding

$$evar = \frac{1}{N\mu_{rc}} \sum_i (\sqrt{(\mathbf{p_i} - \boldsymbol{\mu})^T \mathbf{C^{-1}} (\mathbf{p_i} - \boldsymbol{\mu})} - \mu_{rc})^2 \quad (6)$$

$$\mu_{rc} = \frac{1}{N}\sum_i \sqrt{(\mathbf{p_i} - \boldsymbol{\mu})^T \mathbf{C^{-1}} (\mathbf{p_i} - \boldsymbol{\mu})}$$

B. Polar Euclidean Distance

The Euclidean distances from the nose tip sampled at multiple angles creates a feature vector describing the appearance of a facial curve. From each curve a set of polar distances, d_i, are measured by finding the intersection of rays going out from nose tip at sampling intervals $\Delta\theta = 3^o$ with the facial curve C (Fig. 4). The polar distance signature extracted from each curve is saved in a 120 dimensional feature vector d_i and used for recognition as explained in subsequent sections.

V. EXPERIMENTAL RESULTS

The performance of the curve-based face recognition algorithms proposed in this paper are evaluated using identity verification scenario [14]. A well-known example of verification set-up is an access control system to a secure building where users claim their identity by entering their username or swiping their smart cards. Access control system then captures user's biometric traits (in this case a 3-D scan of the face) and compare this fresh biometric instance with those from the claimed identity stored in the gallery. Access is granted if the biometrics in the probe example and gallery instances are more similar than a required threshold level.

A. Data

A collection of 1196 range images from 119 individuals has been used in this research. This dataset is collected using a stereo imaging system made by 3Q Technologies Ltd. (Atlanta, GA). Arrangements are being made to make this dataset publicly available in near future. In this dataset the pose problem is solved by orienting each unknown face against a generic face located at a standard position in 3-D space using the iterative closest point (ICP) algorithm. All images of the dataset are of size 751×501 pixels. The pixel spacing is 0.32 mm in X, Y, and Z. The "box" containing the face is 160 mm (500 pixels) wide, 240 mm (750 pixels) tall, and 82 mm (256 gray levels) deep. One advantage of this dataset is that all subjects were asked to stand at a specific distance from the sensor and hence all captured 3-D face images are true to size. This dataset includes neutral and expressive faces from subjects belonging to various racial, age, and gender groups.

We partitioned this dataset into two disjoint training and test sets. The training set contains 383 grayscale range images of 10 subjects. The number of images per subject varies between 25 and 47 in the training set. The training set is used to enroll the subjects in the identity authentication experiment. The test set has 389 images from the 10 enrolled subjects (for whom the access should be granted) in addition to 424 extra images from 109 subjects without access privilege (the impostors).

B. Euclidean Distance Decision Rule

As explained in section III, 3-D faces in the dataset are represented either by a set of 3 iso-geodesic or 3 iso-depth curves. Polar distance signatures extracted form each single curve produce a 120 dimensional real-valued feature vector. Simple shape descriptors extracted from facial curve trios (iso-geodesic or iso-depth) are also concatenated to make a 15 dimensional feature vector.

Fisher's LDA is used to independently project the polar distance feature vectors or the shape descriptor features to 9 dimensional feature spaces (lower dimension) that maximize the between-class scatter, S_b, while minimizing the within-class scatter, S_w. The projection directions were learned only from the training portion of the dataset. The features of the images in the test set were projected into the lower dimensional space using the projection parameters learned from the training set.

A Euclidean distance verifier performs identity authentication by comparing the retrieved features of the claimed identity (from the dataset) with the currently captured features of the user and decides whether a match can be declared. This decision is made based on the Euclidean distance between the currently captured features of that individual and the mean

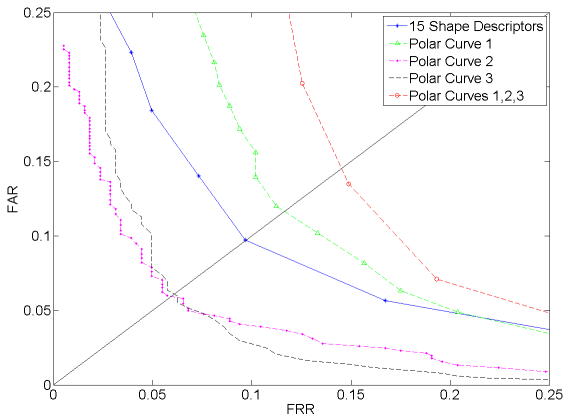

Fig. 5. ROC of Euclidean distance verifier using iso-depth based features.

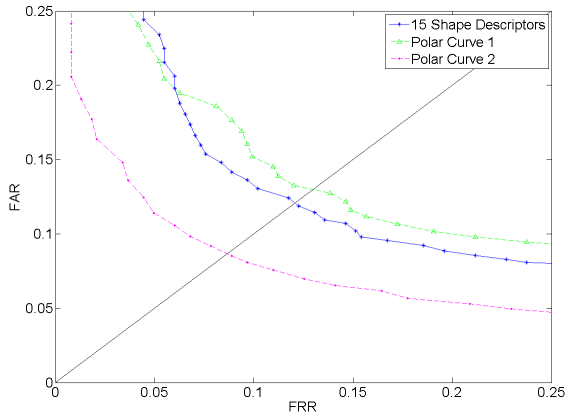

Fig. 7. ROC of SVM using iso-depth based features.

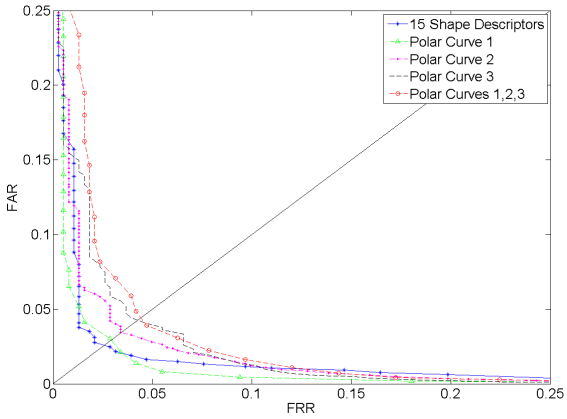

Fig. 6. ROC of Euclidean distance verifier using iso-geodesic based features.

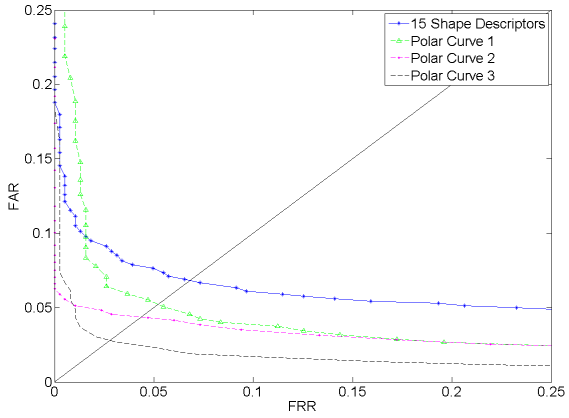

Fig. 8. ROC of SVM using iso-geodesic based features.

value of the features corresponding to claimed identity in the lower dimensional space.

In this paper, the verification performance is evaluated using receiver operating characteristic (ROC) curves and equal error rate (EER) values. Fig. 5 presents the ROC curves of Euclidean distance classifiers trained with various feature combinations extracted from the iso-depth curves. Fig. 6 shows the ROC curves of Euclidean distance verifier using various features extracted from the iso-geodesic curves. Summary of the resulted EER values for both curve types is given in Table I. It is evident that the performance of any combination of iso-geodesic based features outperforms the performance of its iso-depth counterpart. This results confirm our expectation that iso-geodesic curves are more robust against pose variations present in the dataset. Table I shows that the Euculidean distance decision rule using features extracted from iso-geodesic curves can achieve a remarkable performance of EER$= 2.58\%$.

TABLE I

EER PERCENTAGE OF EUCLIDEAN DISTANCE VERIFIER ACROSS VARIOUS FEATURE SETS

Euclidean Distance Classifier		
	iso-geodesic	level-set
Shape Descriptors	2.58%	9.07%
Polar distance of first curve	2.93%	11.6%
Polar distance of second curve	3.44%	5.9%
Polar distance of third curve	4.25%	6.1%
Polar distance of all three curves	4.42%	14%

C. Support Vector Machine

The identity verification problem explained in this project is solved by decomposition to 10 binary problems for which the standard one-against-all (1-a-a) SVM is used. In the training phase 10 decision functions $f_m(x),\ m \in K = \{1, \ldots, 10\}$ are constructed, where the rule $f_m(x)$ separates the training data of the m-th class from the rest of training data. The request of a user with biometric features x claiming the identity of class m is accepted only if the value of function $f_m(x), m \in K$ is more than a predefined threshold. In this paper we have only experimented with linear SVM kernels. Investigation of polynomial and Gaussian kernels are left for future works.

Fig. 7 presents the ROC curves of linear 1-a-a SVMs trained with various feature combinations extracted from iso-depth curves. Fig. 8 show the ROC curves of linear SVMs

TABLE II
EER PERCENTAGE OF SVM CLASSIFIER ACROSS VARIOUS FEATURE SETS

SVM		
	iso-geodesic	level-set
Shape Descriptors	6.82%	12.08%
Polar distance of first curve	5.22%	12.98%
Polar distance of second curve	4.36%	8.67%
Polar distance of third curve	2.79%	6.81%

using various features extracted from iso-geodesic curves. Table II summarize the resulted EER values for both curve types. Again, it is interesting to note that the performance of any combination of iso-geodesic based features is better than its iso-depth counterpart. This confirms the inherent robustness of iso-geodesic curves against pose variations present in the dataset. Table II shows that SVM classifiers benefiting from features extracted from iso-geodesic curves can achieve a remarkable performance of EER$= 2.79\%$.

VI. CONCLUSION

In this paper we introduced novel 3-D face recognition algorithms based on curves extracted from facial surfaces. Their verification performance is reported and compared using a dataset of 1196 range images of expressive and neutral faces. The observed verification accuracies show the highly competitive performance of our algorithm relative to existing face recognition algorithms. For example, Pan *et al.* [15] has investigated using a PCA-based approach and a Hausdorff distance approach for 3-D face recognition. They have evaluated their algorithms using a dataset of 360 range images from 30 individuals and reported EER in the range of $3-5\%$ for the Hausdorff distance approach and EER in the range of $5-7\%$ for PCA-based approach.

Mpiperis *et al.* [6] have proposed a 2D+3D face recognition algorithm where facial expression in both range and portrait representation of the face is compensated using the geodesic polar parameterization of facial surface. They have tested their algorithm on a database of 1500 images from 100 subjects and reported EER in the range of $4.9-15.4\%$.

Reviewing these results highlights the effectiveness of proposed curve-based facial representations in capturing discriminating facial biometrics. We have shown that by using simple shape descriptors extracted from iso-geodesic curves, verification performance can be significantly improved and EER values as low as 2.58% are achiveable.

By comparing the results shown on tables I and II it appears that LDA followed by Euclidean distance verifier outperforms SVM. This is because we are merely using linear SVM. The next logical step to improve the performance is to use non-linear SVMs (Gaussian and polynomial kernels). Another choice is using iso-geodesic curves extracted from around other fiducial points like eye corners. Finally, we are seeking ways to combine decisions of different classifiers.

REFERENCES

[1] R. Hammoud, B. Abidi, and M. Abidi, *Face Biometrics for Personal Identification: Multi-sensory Multi-modal Systems*. Springer, 2007.

[2] Bachelor of science in biometric systems, west virginia university. [Online]. Available: http://www.lcsee.cemr.wvu.edu/ugrad/degree-info.php?degree=bsbs

[3] (2006) Biometrics history. [Online]. Available: http://www.biometrics.gov/Documents/BioHistory.pdf

[4] K. W. Bowyer, K. Chang, and P. Flynn, "A survey of 3d and multi-modal 3d+2d face recognition," Notre Dame Department of Computer Science and Engineering Technical Report., Tech. Rep., January 2004.

[5] P. Phillips, P. Grother, R. Micheals, D. Blackburn, E. Tabassi, and J. Bone, "Face recognition vendor test 2002," National Institute of Standards and Technology, Tech. Rep., 2003. [Online]. Available: www.frvt.org

[6] I. Mpiperis, S. Malassiotis, and M. G. Strintzis, "3-d face recognition with the geodesic polar representation," *Information Forensics and Security, IEEE Transactions on*, vol. 2, no. 3, pp. 537–547, Sept. 2007.

[7] C. Chua, F. Han, and Y. Ho, "3D human face recognition using point signature," *Proc. 4th IEEE Int. Conf. on Automatic Face and Gesture Recognition*, vol. 1, pp. 233–238, 2000.

[8] C. Samir, A. Srivastava, and M. Daoudi, "Three-Dimensional Face Recognition Using Shapes of Facial Curves," *IEEE TRANSACTIONS ON PATTERN ANALYSIS AND MACHINE INTELLIGENCE*, pp. 1858–1863, 2006.

[9] Y. Sun and M. Abidi, "Surface matching by 3d point's fingerprint," in *Computer Vision, 2001. ICCV 2001. Proceedings. Eighth IEEE International Conference on*, vol. 2, 7-14 July 2001, pp. 263–269vol.2.

[10] M. Peura and J. Iivarinen, "Efficiency of simple shape descriptors," *Aspects of Visual Form*, pp. 443–451, 1997.

[11] J. Milnor, *Morse Theory*. Princeton University Press, 1963.

[12] S. Jahanbin, A. C. Bovik, and H. Choi, "Automated facial feature detection from portrait and range images," *IEEE Southwest Symposium on Image Analysis and Interpretation*, 2008.

[13] R. Kimmel and J. Sethian, "Computing geodesics on manifolds," *Proceedings of NatŠl Academy Sciences*, pp. 8431–8435, 1998.

[14] H. Moon and P. Phillips, "The FERET verification testing protocol for face recognitionalgorithms," *Automatic Face and Gesture Recognition, 1998. Proceedings. Third IEEE International Conference on*, pp. 48–53, 1998.

[15] G. P. Z. W. Y. Pan, "Automatic 3d face verification from range data," *Acoustics, Speech, and Signal Processing, 2003. Proceedings. (ICASSP '03). 2003 IEEE International Conference on*, vol. 3, pp. III–193–6 vol.3, 6-10 April 2003.